

# A PFG NMR Self-Diffusion Investigation of Probe Diffusion in an Ethyl(hydroxyethyl)cellulose Matrix

Magnus Nydén,<sup>\*,†</sup> Olle Söderman,<sup>†</sup> and Gunnar Karlström<sup>‡</sup>

Department of Physical Chemistry 1 and Theoretical Chemistry, Center for Chemistry and Chemical Engineering Box, 124, University of Lund, S-221 00 Lund, Sweden

Received July 7, 1998; Revised Manuscript Received October 14, 1998

**ABSTRACT:** The translational dynamics of poly(ethylene oxide) (PEO), in ethyl(hydroxyethyl)cellulose (EHEC) solution and in a chemically cross-linked gel of EHEC, is investigated by means of pulsed field gradient (PFG) NMR. Two different matrix concentrations of EHEC are studied, 1 and 6 wt % in which the PEO concentrations are 0.01 and 0.06 wt %, respectively. The molar mass of PEO is varied from  $10^4$  to  $10^6$ , and they are fairly monodisperse (typically  $M_w/M_n < 1.1$ ). The echo decays for the PEO in the 1% EHEC solution show Gaussian diffusion behavior as indicated by straight lines when the echo intensities are plotted vs the relevant parameters. This is also the case for PEO diffusing in the 6% EHEC solution matrix. For PEO diffusing in the 1% EHEC gel, a more complex situation is at hand. This is indicated by the observation of nonlinear echo decays for the PEO. The molar mass dependence of the mean-square displacement is compared to scaling relations ( $\langle z^2 \rangle = KM^{-\alpha}$ ) and to computer simulations by Baumgärtner and Muthukumar for heterogeneous systems. For the 1% EHEC solution and gel, the  $\langle z^2 \rangle$  dependence on the molar mass shows power law scaling with  $\alpha \approx 1$ . For the case when the EHEC solution matrix is 6%, a more complex behavior is seen, as revealed by a different functional form for the  $\langle z^2 \rangle$  dependence on the molar mass. These observations are discussed in terms of polymer diffusion inside a heterogeneous matrix.

## Introduction

Ethyl(hydroxyethyl)cellulose is a water-soluble polymer with interesting solution properties. The static and dynamic properties of mixtures of EHEC with surfactants, cosolutes, and other polymers have been extensively investigated in earlier papers.<sup>1–13</sup> However, the diffusion processes and the solution structure of EHEC in water are still not fully understood. In a recent paper we presented an NMR self-diffusion study of EHEC in water solutions.<sup>14</sup> The results indicated a wide spread of diffusion coefficients for the polymer molecules. We argued that this spread was most likely due to the self-aggregating properties of the polymer. However, the true mechanism for the spread of diffusion coefficients could not be elucidated. (The fact that the aggregates are required to be long-lived on the time scale of the experiment points to aggregates with surprisingly long lifetime.) The possibility of a strong molar mass scaling of the diffusion coefficient, due to matrix heterogeneities, could not be ruled out.

In this work we have further developed the ideas discussed in the previous paper<sup>14</sup> by studying the diffusion of small amounts of monodisperse probe polymers in EHEC solutions and gels. The probe molecules used were poly(ethylene oxide) (PEO)<sup>34</sup> since it has been shown from cloud point measurements that the presence of  $C_{12}E_5$  in water solutions of EHEC does not affect the cloud point or the viscosity.<sup>32</sup> In addition, the polymer is available with a wide range of molar masses with narrow size distributions.

We note that polymer diffusion is an active area of research. PFG NMR is a very important method in measuring the self-diffusion coefficient of both polymers

and smaller molecules in the presence of polymer matrixes. It is our belief that when the diffusion behavior of the probe and/or the polymer matrix is complicated, much information can be found in the functional form of the echo decay. In addition, the scaling behavior in complex self-associating systems has been found to differ from that in homogeneous systems. Thus, we believe that there is a need for accurate data in the development of the theory in this field.

The aim of this work is to investigate the molar mass scaling of the PEO diffusion coefficient in a EHEC matrix. We will provide accurate data concerning the scaling coefficients and the functional form of this scaling. In addition, we report on the functional form of the echo decay (which is indicative of diffusion in heterogeneous media) for PEO diffusing in a covalent gel of EHEC.

## Experimental Section

**Materials.** The EHEC polymer (Figure 1) was obtained from Akzo Nobel Surface Chemistry AB, Stenungsund, Sweden. This particular type of EHEC has a degree of substitution of ethyl and hydroxyethyl groups of 0.6–0.7 and 1.8, respectively (values quoted by the manufacturer). The average molecular weight for this type of EHEC is approximately 100 kDa. Before use, EHEC was dissolved in water, and impurities that were not soluble in water were removed by centrifugation at 10 000 rpm. The clear phase was dialyzed against Millipore water until the conductivity decreased below 2 mS/m. The sample was then freeze-dried to give the purified product. PEO with molar masses 10, 18, 32, 50, 73, 120, 205, 288, 645, and 963 kDa were purchased from Polymer Laboratories and used as received. The polymer standards had narrow size distribution, typically  $M_w/M_n < 1.1$ .  $D_2O$  was purchased from Dr. Glaser, AG Basel. Three different stock solutions of EHEC were prepared: 1% solution, 1% gel, and 6% solution. For each stock solution, 10 samples were prepared with the different molar masses of PEO. In total 30 samples were prepared by

\* To whom correspondence should be addressed.

<sup>†</sup> Department of Physical Chemistry 1.

<sup>‡</sup> Department of Theoretical Chemistry.

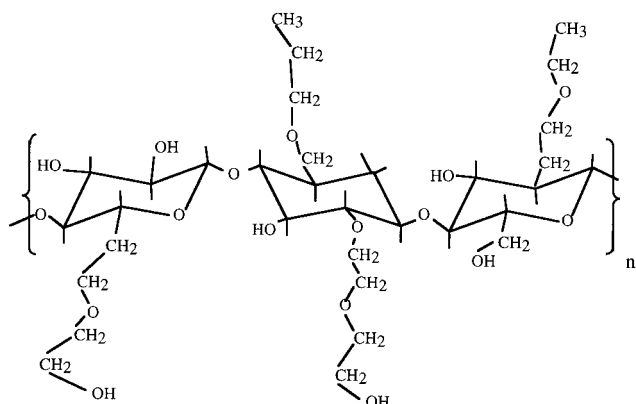


**Figure 1.** Chemical structure of EHEC. Note that this is not an exact structure but merely represents one of the many different ways for the substituents to be attached to the cellulose backbone.

mixing standard solutions of EHEC and PEO. The solutions were equilibrated by slowly tilting back and forth for 50 h. The EHEC gel samples were prepared by a method developed by Rosén et al.<sup>16</sup> The cross-linking reagent was DVS (divinyl-sulfone). The 1% EHEC solution was allowed to react with DVS under basic conditions (0.02 M NaOD) to produce the chemically cross-linked gel. The concentrations of PEO were chosen to 0.01% and 0.06% for the 1% and 6% EHEC, respectively. These concentrations were chosen in order to work below the overlap concentration for the pure PEO system for all molar masses.

## Theoretical Background

**NMR Self-Diffusion.** The PFG NMR self-diffusion experiment is an important tool for the measurements of self-diffusion coefficients for freely diffusing species in both solutions and other types of matter. In addition, due to recent development in both theory (the introduction of the  $q$ -space concept) and hardware (stronger field gradients), it is possible to probe the microstructure in systems where the diffusion is not free but restricted in some way. In the latter type of experiment one powerful tool is to use the concept of  $q$ -space<sup>17</sup> in analogy with scattering techniques such as the neutron spin-echo experiment. The echo decay  $E(\vec{q}, \Delta)$  is then described by<sup>18</sup>

$$E(\vec{q}, \Delta) = \int P(\vec{R}, \Delta) \exp(i2\pi\vec{q} \cdot \vec{R}) d\vec{R} \quad (1)$$

Here  $P(\vec{R}, \Delta)$  is the average propagator, where  $\vec{q} = \gamma\vec{g}\delta/2\pi$  is the magnetogyric constant for protons,  $\delta$  is the field gradient pulse length,  $g$  is the field gradient strength, and  $\Delta$  is the effective diffusion time. In this work, a Hahn echo was used with  $\Delta = 140$  ms; typical values of  $\delta$  ranged between 0.5 and 10 ms depending on the molar mass and concentration.  $g$  was normally varied from 0 to 6 T/m.

Equation 1 shows the Fourier relationship between the average propagator, which contains the translational dynamic information, and the echo decay. One nice example is the PFG NMR experiment performed on water diffusing between packed polystyrene spheres.<sup>19</sup> Due to the repeating structure, the echo decay for water shows typical coherence effects in which the inverse  $q$  value of the peak is related to the length scale probed in the PFG NMR experiment.

If the diffusion is nonrestricted,  $P(\vec{R}, \Delta)$  is a Gaussian function. It is then possible to relate eq 1 to the diffusion

coefficient according to

$$E(q, \Delta) = \exp(-4\pi^2 q^2 D \Delta) \quad (2)$$

where  $2D\Delta = \langle z^2 \rangle$  is the mean-square displacement. If  $\log(E)$  is plotted against  $q^2$  (from here on referred to as a Stejskal–Tanner plot), a straight line is obtained. If the diffusion of the molecules is more complex, the propagator is no longer Gaussian. However, it is still possible to measure the mean-square displacement by expanding eq 2 in a Taylor series. One obtains

$$E(q) \approx 1 - 4\pi^2 q^2 \langle z^2 \rangle + O(\langle z^4 \rangle) \quad (3)$$

In addition, we note the possibility of non-Fickian diffusion. This is manifested in the mean-square displacement dependence of diffusion time,  $\Delta$ , according to

$$\langle z^2 \rangle \propto \Delta^\mu \quad (4)$$

with  $\mu = 2/d_w$ , where  $d_w$  is the fractal dimension of the random walk. There may be several reasons for such behavior. In this paper we have specifically been interested in the earlier results by Walderhaug et al.<sup>15</sup> that indicated fractal diffusion of EHEC as shown by the PFG NMR method. However, in this work no such fractal diffusion has been noticed from a variation of the experimental diffusion time. We have varied the time scale between 140 and 560 ms and have not detected any time dependence in the diffusion coefficient.

In what follows we choose to calculate  $\langle z^2 \rangle$  for all echo decays. For the cases when the echo decays can be evaluated by eq 2,  $\langle z^2 \rangle$  will be calculated according to  $\langle z^2 \rangle = 2D\Delta$ . When eq 2 cannot be used to describe the echo decay data,  $\langle z^2 \rangle$  will be evaluated from the initial slope of the data according to eq 3.

**Obstruction Models.** The diffusion coefficient of a molecule diffusing in a matrix of polymers will depend on the obstruction effect exerted on the probe by the matrix. If the probe is a polymer, the diffusion coefficient dependence on the molar mass is often expressed as<sup>20</sup>  $\langle z^2 \rangle = KM^{-\alpha}$ . If the matrix concentration is low,  $0.5 < \alpha < 0.6$ . When the concentration of the matrix and/or the molar mass of the probe increases, the scaling exponent  $\alpha$  will increase, and in the case of very strong topological constraints (the so-called reptation model),  $\alpha = 2$ . In addition, Muthukumar et al.<sup>21–23</sup> have shown that the functional form of the relation between the mean-square displacement and the molar mass can provide a guide for separating homogeneous and heterogeneous media. By means of computer simulations, they showed that in a certain molar mass regime,  $\alpha$ , increased from 2 to 3 when heterogeneities were introduced in the system. This value of  $\alpha$  is to be compared with the Rouse regime for which  $\alpha = 1$  and the reptation regime for which  $\alpha = 2$ .

In this work, the lowest concentration of matrix polymer (EHEC) is about 5 times the overlap concentration. Previous work has shown that, in order to reach scaling exponents close to the reptation value of 2, high molecular weight polymers at high concentrations have to be used. In this work the average molar mass of EHEC is only 100 kDa. It is not clear that the dominant diffusion mechanism will be the reptation mechanism. Considering the low volume fraction of EHEC, one

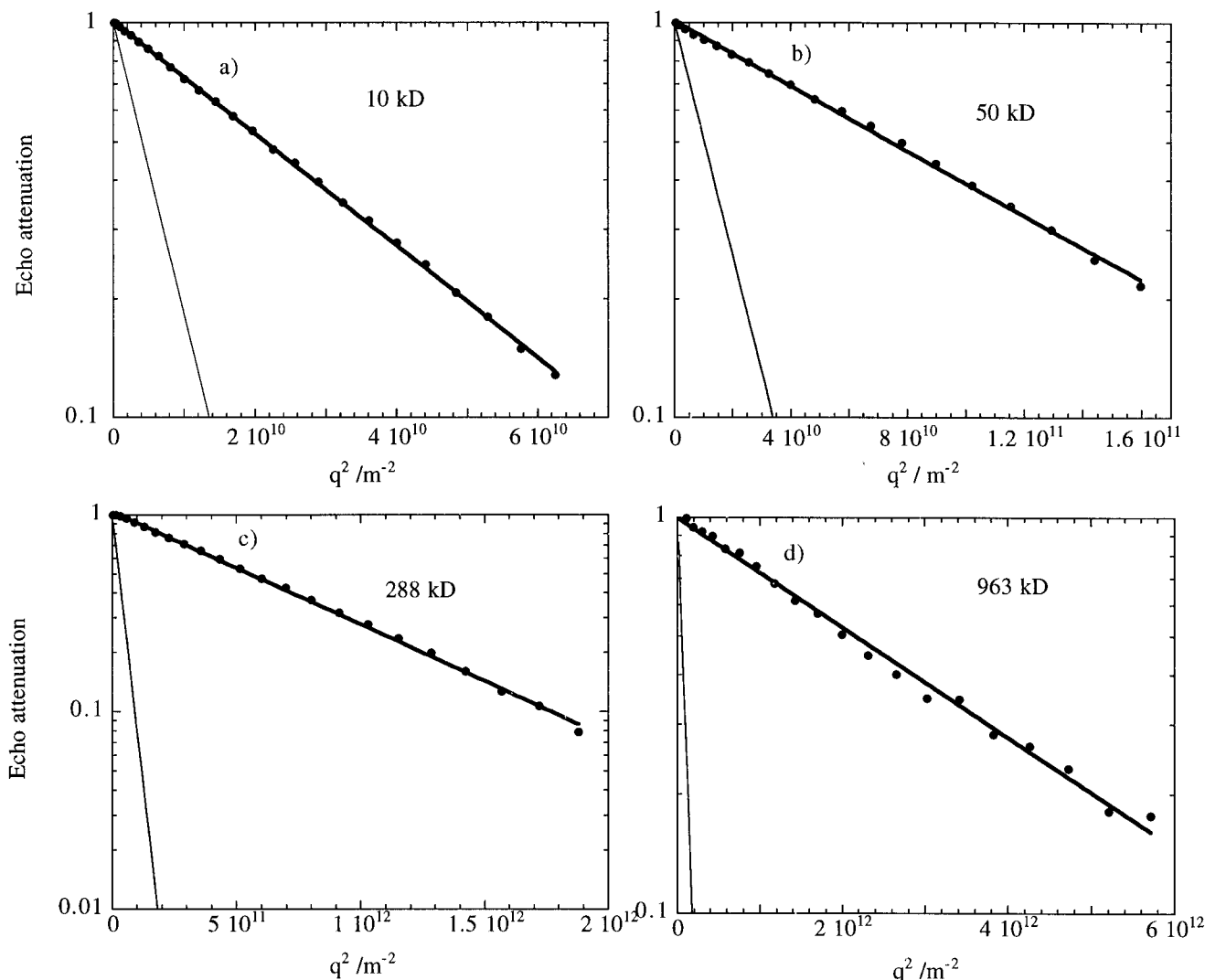


**Figure 2.** Stejskal-Tanner plot of echo decay for the different PEO's in 1% EHEC solution. Note that for Gaussian diffusion the result is a straight line in this type of representation. The full line is a fit of eq 2 to the data. (a) 10, (b) 50, (c) 288, and (d) 963 kDa. The thin line is the echo decay for the corresponding molar mass of PEO without the presence of EHEC.

possible diffusion mechanism for PEO is free diffusion in solution, slightly hindered by the EHEC matrix.

One way to quantify the diffusion data in this case is to use the model by Johansson et al.<sup>24</sup> They showed that the diffusion coefficient of a hard sphere in a matrix could be written as

$$D/D_0 = \exp(-\alpha) + \alpha^2 \exp(\alpha) E_1(2\alpha) \quad (5)$$

where  $\alpha = \phi_p(R_s + a)^2/a^2$ .  $\phi_p$  is the volume fraction of the obstructing polymer,  $R_s$  is the radius of the probe,  $a$  is the radius of the matrix forming polymer,  $D_0$  is the diffusion coefficient without the matrix present, and  $E_1$  is the exponential integral  $E_1(x) = \int_x^\infty \exp(-n)/n \, dn$ . It should be mentioned that eq 5 is strictly valid for small "hard" molecules diffusing in a matrix. In effect, this means that when the dimensions of the probe molecule and the matrix network are of the same magnitude,  $D/D_0$  will take on very small values, indicating a near total obstruction of the diffusing particle. For the case when the probe is a polymer, the diffusion mechanism will change from hard-sphere character to "polymer"-like motion, the nature of which is determined by the topological constraints of the network. It thus becomes apparent that eq 5 at most can describe the initial part of the  $\langle z^2 \rangle$  dependence on the polymer radius.

In addition, it has been shown that the diffusion coefficient of a dilute Brownian probe in a polymer matrix can be written according to<sup>25</sup>

$$D/D_0 = \exp(-\kappa R) \quad (6)$$

where  $R$  is the radius of the probe and  $\kappa^{-1}$  is the screening length of the semidilute polymer matrix.  $D_0$  has the same meaning as in eq 5. It should be noted that we expect eq 6 to be of use for the low molar mass PEO. The reason being that at low molar masses the self-diffusion behavior of the probe is expected to follow a hard-sphere type relation, where the dynamics is to a large extent given by hydrodynamic interactions and consequently follows the functional form of eq 6. However, as the molar mass increases, the topological constraints from the matrix increases, and the functional form of eq 6 will most likely not describe the data due to a change in diffusion mechanism.

## Results

**1% EHEC Solution Matrix.** In Figure 2 a-d the echo decays for four different molar masses of PEO diffusing in the 1% EHEC matrix are shown. In addi-

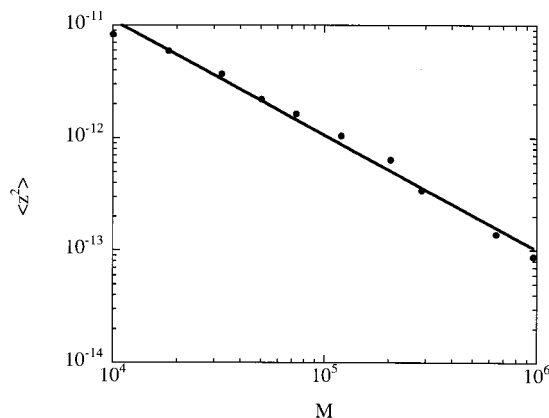


**Figure 3.** Mean-square displacement for the 1% EHEC solution case vs the molar mass  $M$ .  $\langle z^2 \rangle$  was evaluated according to eq 2. The full line is a fit to  $\langle z^2 \rangle = KM^{-\alpha}$ .

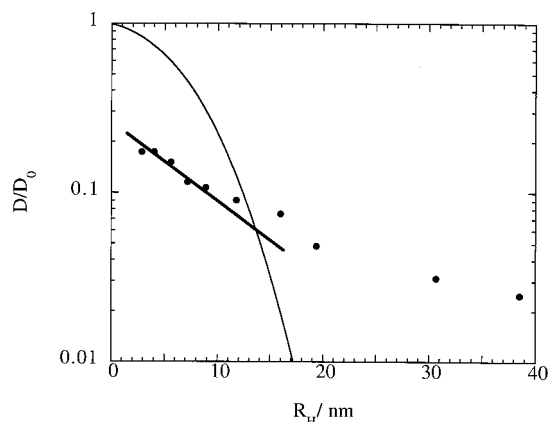


**Figure 4.** Plot of  $D/D_0$  is the diffusion coefficient, normalized with the diffusion coefficient in the absence of matrix, vs the radius of the PEO. The thin line is a fit of the theory by Johansson et al. according to eq 5. The thick line is a fit of eq 6 to the first five molar masses of PEO.

tion, data for the PEO echo decay without the presence of the polymer matrix (EHEC) are presented.

Interesting to note is that with only 1% EHEC the obstruction of the PEO is quite severe, as can be noted in the difference in the slope of the echo decays. For all molar masses the echo decay follow Gaussian behavior when plotted in a Stejskal–Tanner plot. The straight lines are fits of eq 2.

The result of applying the scaling relation  $\langle z^2 \rangle = KM^{-\alpha}$ , is shown as a full line in Figure 3. The scaling exponent  $\alpha = 0.96$ . One interesting feature about Figure 3 is that  $\langle z^2 \rangle$  is reduced by a factor 3 in comparison with  $\langle z^2 \rangle$  for PEO without EHEC present in the matrix. Taking into account that the EHEC concentration is only 1% and that the concentration of PEO itself is much lower than the overlap concentration, this is a very strong obstruction effect.

In Figure 4,  $D/D_0$  is shown vs  $R_H$  (hydrodynamic radius) according to  $R_H = K'M^\mu$ .  $K'$  is taken from ref 33 and  $\alpha$  is 0.53.  $D_0$  is the diffusion coefficient of PEO without EHEC present. The line is a fit of eq 6 to the low molar masses. Equation 6 describes the data well at low molar mass PEO, and consequently we use this to calculate the dynamical screening length of the 1% EHEC matrix. The result is  $\kappa^{-1} = 15$  nm. The prediction of eq 5 is shown in Figure 4. It is clear that it fails to account for the data. As mentioned previously, this behavior is expected due to the underlying derivation of eq 5.

**1% EHEC Gel Matrix.** In Figure 5 a–d representative echo decays for different molar masses of PEO diffusing in the 1% EHEC gel matrix are shown.

Starting with the echo decay for the 10 kDa PEO, the data are reasonably well described by a straight line in the Stejskal–Tanner representation. However, the residuals indicate that the echo decay is in fact slightly curved. The effects is more pronounced for the 18 kDa PEO, where the echo decay clearly deviates from linear behavior. The effect becomes more and more pronounced as the molar mass increases. As evident in Figure 5d, the echo decay for the highest molar mass (963 kDa) shows a complex behavior. It is not possible to fit a biexponential decay to the data. If we compare the initial slope of the echo decays for PEO in the presence of EHEC gel with PEO diffusing in pure water solution, it appears as if there exists a fraction of PEO in the gel that experiences only small obstruction. At higher  $k$  values there also appears to exist a fraction that shows evidence of very strong obstruction.

In Figure 6, the results for  $\langle z^2 \rangle$  as function of  $M$  are shown.  $\langle z^2 \rangle$  was evaluated according to eq 3. From the fit of a power law according to  $\langle z^2 \rangle = KM^{-\alpha}$ , it is clear that  $\langle z^2 \rangle$  displays a power law dependence with  $\alpha \approx 0.9$ . The fact that the mean square displacement differs between the gel and solution requires some comments on the evaluation procedure. In Figure 3, the evaluated mean-square displacement is common for all PEO molecules as indicated by the straight line in a Stejskal–Tanner plot. For the PEO diffusing in the gel matrix (Figure 6) the mean-square displacement was evaluated from the initial slope. Consequently, if the reason for the deviation from a straight line is the fact that the propagator is not Gaussian, the evaluated mean-square displacement is correct. However, if the curvature in the echo decay is due to a spatially heterogeneous matrix, the evaluated mean-square displacement is weighted by the fast diffusing species. This may explain the small difference in  $\langle z^2 \rangle$  between the solution and gel case.

**6% EHEC Solution Matrix.** When increasing the EHEC concentration to 6%, there is a clear change in the diffusion behavior of PEO as compared to the 1% case as seen in Figure 7. In actual fact, data for most of the molar masses are well described by a single diffusion coefficient (Gaussian propagator). However, when the molar mass exceeds 288 kDa, the echo decay data can no longer be described with one diffusing component. In contrast to the echo decay for PEO in the 1% EHEC solution and gel matrixes, the data are rather well described with a biexponential decay. The echo decay, along with the relevant fitting function for the same molar masses as shown for the 1% EHEC samples, is shown in Figure 7a–d. Noting that it is only for the highest molar mass PEO that the fraction of fast diffusing species becomes significant, we show the result from the evaluation of  $\langle z^2 \rangle$  vs  $M$ , where  $\langle z^2 \rangle$  is taken to be the slowly diffusing component in the biexponential echo decay. The results are shown in Figure 8. Note that the quality of the data is much better than for the 1% EHEC, due to the higher concentration of PEO. To investigate whether non-Fickian diffusion occurs, we measured the mean-square displacement of the highest molar mass of PEO as a function of time. Three times were chosen, 0.14, 0.28, and 0.56 s. The result is shown in Figure 9, and from the fit of eq 4, we note that  $\mu = 1$ . This indicates that the self-diffusion is governed by



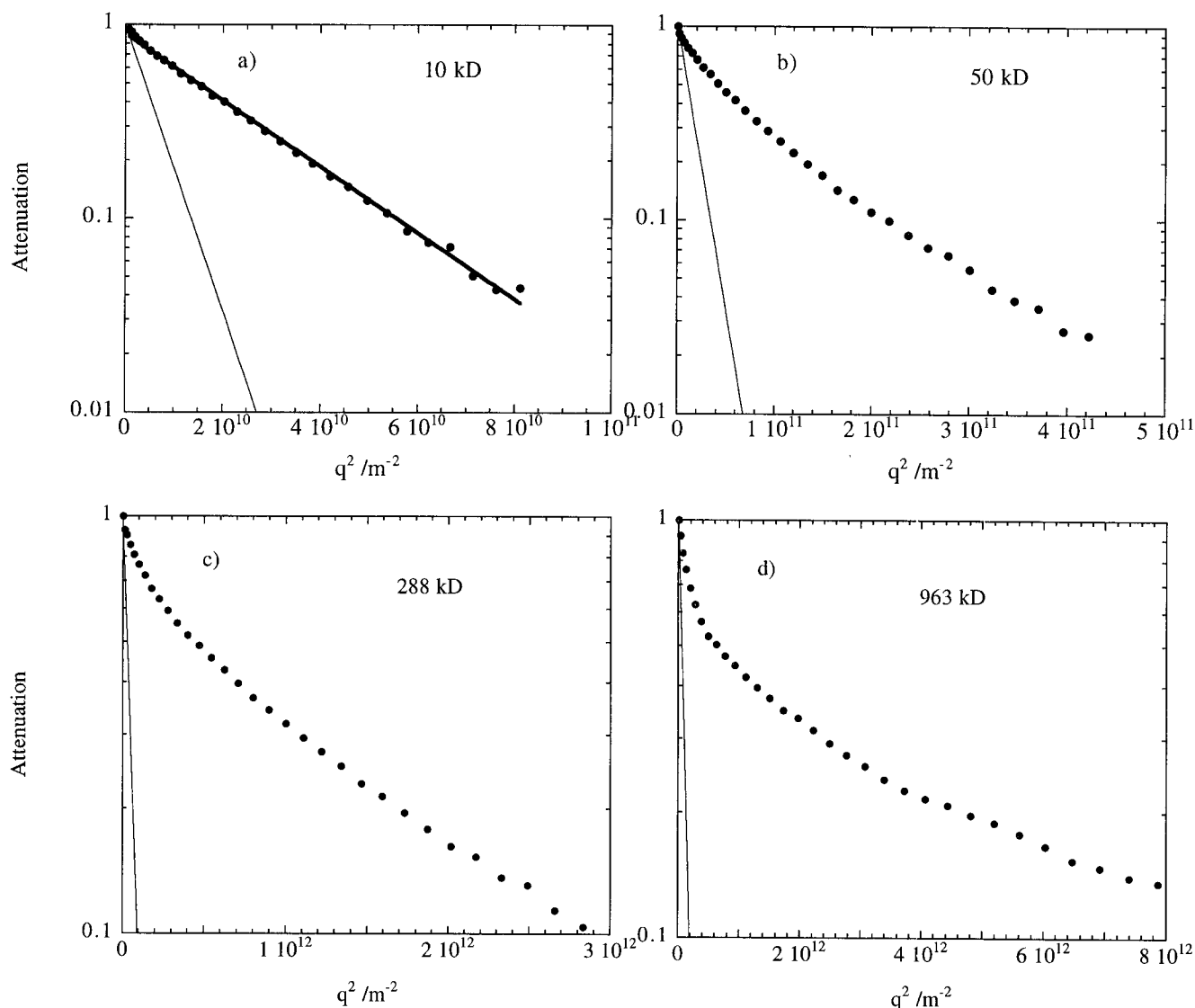


**Figure 5.** Echo decays for different molar masses of PEO diffusing in 1% EHEC gel. The same molar masses of PEO were chosen as for the case of the 1% EHEC solution. The plots are all represented as Stejskal–Tanner plots. For the 10 kDa (a) PEO the diffusion appears to be Gaussian, but at close examination there is a small curvature in the echo decay. As the molar mass increases, the curvature becomes more pronounced. To evaluate the mean-square displacement, according to eq 3, the first five data points were chosen. The thin line is the echo decay for the corresponding molar mass of PEO without the presence of EHEC.

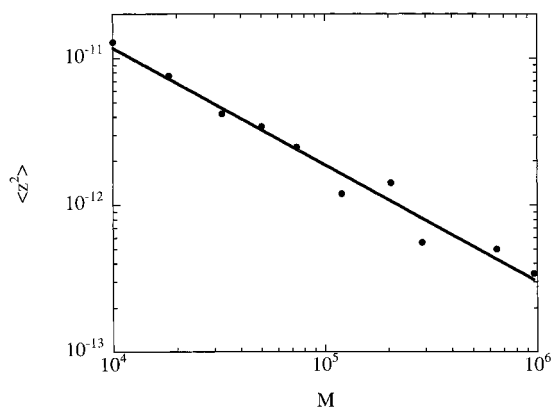


**Figure 6.** Mean-square displacement,  $\langle z^2 \rangle$ , evaluated from the data in Figure 5, vs the molar mass PEO for the 1% EHEC gel matrix. The line is a fit according to  $\langle z^2 \rangle = KM^{-\alpha}$  and gives  $\alpha \approx 0.9$ .

Fickian diffusion. We also note that the results presented here are not in agreement with the results presented by Walderhaug et al.<sup>15</sup>

To make sure that the presence of PEO does not influence the diffusion behavior of EHEC, we performed diffusion experiment for EHEC containing different molar masses of PEO. In Figure 10 the results of these measurements are shown.

The echo decay for EHEC is clearly independent of the molar mass of PEO. In addition, experiments were performed to ensure that the diffusion behavior of PEO was the same in the basic DVS solution as in that of pure water solution, and no significant difference was observed.

## Discussion

**Background.** The dynamic properties of polymers in solution and in the melt constitute an important area of research during the past decades. The area has expanded considerably both experimentally and theoretically. Theoretical frameworks due to de Gennes<sup>26</sup> and Doi and Edwards,<sup>20</sup> that cover both dynamics of concentrated solutions and melts, initiated a number of experimental investigations. In the early stage, most experiments verified the reptation theory by de Gennes

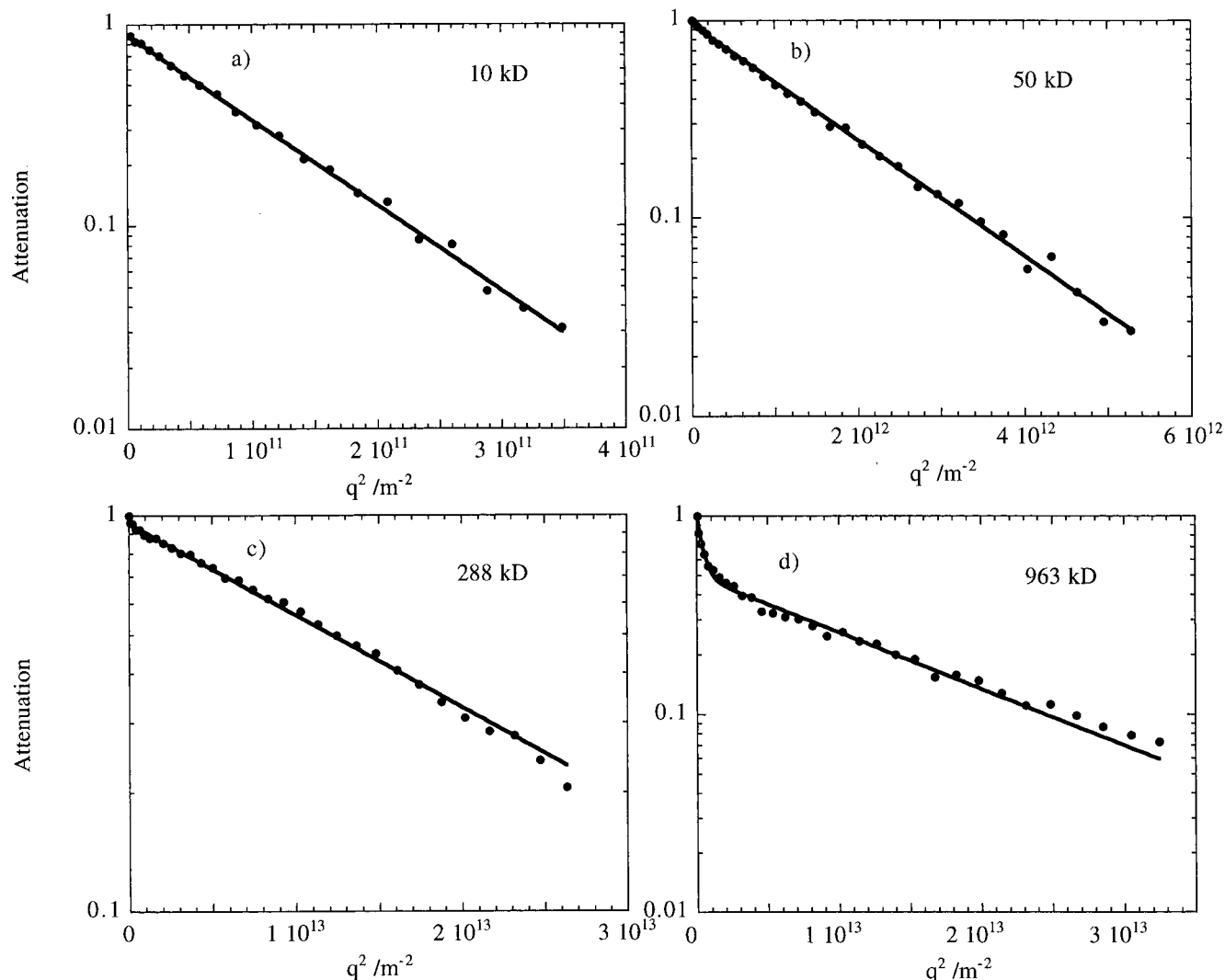


**Figure 7.** Echo decays for different molar masses of PEO diffusing in 6% EHEC solution. The same molar masses of PEO were chosen as for the case of the 1% EHEC solution and 1% EHEC gel. Here the main part of the molar mass range shows Gaussian behavior as seen by the linear echo decay. For the 288 kDa sample (c), the results indicate a second contribution to the echo decay as seen by a fast decay at low  $q$  values. The fraction ( $f$ ) of the second component is smaller than 5%. For the highest molar mass PEO (d) the same effect is seen. However, now the fraction of the fast component is significantly higher, and the fit of a biexponential decay shows that  $f = 0.5$ .

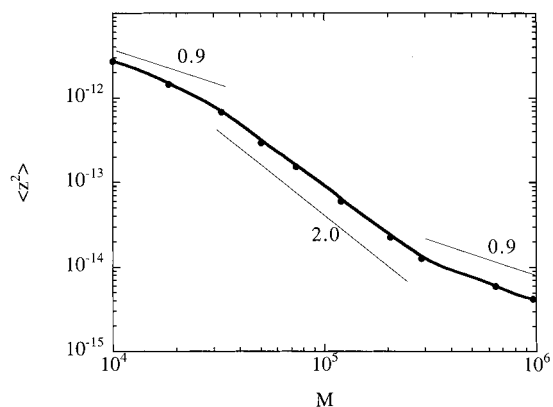


**Figure 8.**  $\langle z^2 \rangle$  vs  $M$  for the PEO diffusing in the 6% EHEC solution. The line is simply a guide for the eye. Shown also is the slope of the curve at some interesting parts on the curve.

and Doi/Edwards. However, as time elapsed, some experimental results in the semidilute regime emerged that were not in accordance with reptation. In particular, it was found that the  $\langle z^2 \rangle = KM^{-2}$  scaling, that followed from the assumption of reptation, was not

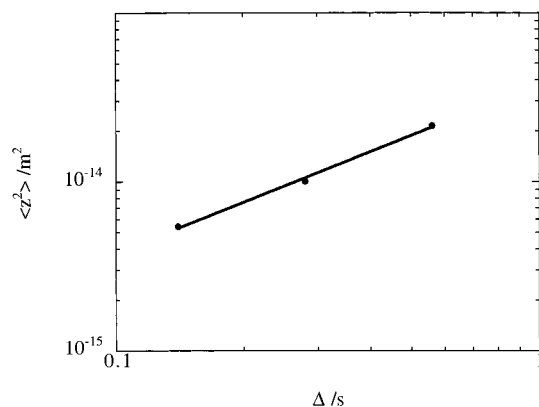


**Figure 9.** Time dependence of the mean-square displacement for the 963 kDa sample in 6% EHEC matrix. The line is a fit of eq 4 to the data, giving  $m = 1$ . This indicates that the diffusion is governed by a Fickian diffusion process. The measurements were limited to three diffusion times only due to a combination of slow diffusion, relaxation, and  $j$ -coupling effects.

always obeyed. Instead, an even stronger scaling with molar mass was obtained. However, for very high

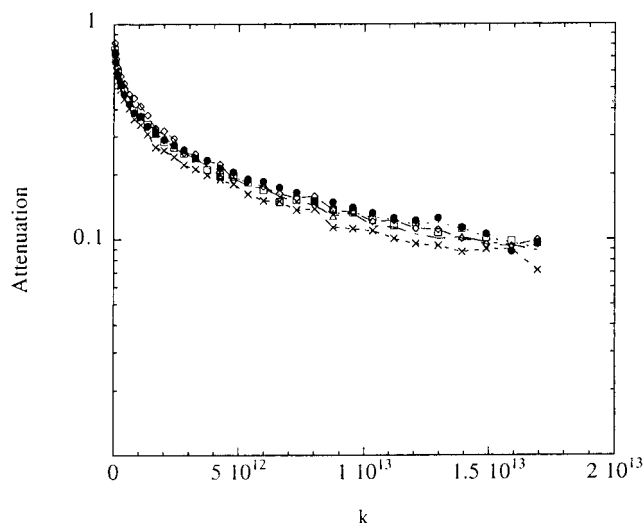


**Figure 10.** Echo decays for EHEC for different molar masses of PEO. The results show that there is no significant change in diffusion behavior of EHEC in samples containing different molar mass of PEO, indicating that the concentration of PEO is below  $c^*$  for the molar mass range investigated. Thus, PEO does not affect the diffusion behavior of EHEC.

concentrations and particularly in the melt, the results were in agreement with reptation, most probably due to the very strong topological constraints.

Important assumptions underlying reptation is the presence of strong topological constraints, but an additional important assumption is that the solution is homogeneous. For polymers with self-associating properties, a heterogeneous structure may be formed. The effect of heterogeneities on diffusion processes was initially investigated by means of computer simulations by Muthukumar and Baumgärtner.<sup>21–23,27</sup> These authors showed that in heterogeneous systems the scaling exponent  $\alpha$  could take on larger values than those reported for reptation. The results were discussed in terms of “entropic trapping” of polymers in pores formed by the polymer matrix. The simulation results were in line with some experimental results.<sup>28,29</sup>

In a recent paper by Slater and Wu,<sup>30</sup> it was shown that heterogeneous environments affected the mechanism of diffusion. In particular, it was shown that a very small amount of heterogeneities was needed to “kill reptation” (in the words by Slater and Wu) and that the effect of entropic trapping was introduced when the matrix concentration represented the percolation threshold in the system.

The papers discussed above treat systems with high concentrations and high molar masses (an assumption for the reptation model to apply). In this study, the highest concentration of EHEC is 6%. This is far above the overlap concentration. However, considering the results from previous papers,<sup>28,29</sup> this concentration is most likely not high enough for the reptation model to apply. However, the results from computer simulations on entropic trapping of polymers would appear to apply. In what follows we will describe in more detail the experimental results concerning the echo decays and point out the resemblance between the scaling results found here and those found in the models by Muthukumar and Baumgärtner and by Slater and Wu.

**Experiments.** Starting with the 1% EHEC solution we note that the echo decay data indicate that the diffusion behavior of the PEO probes is Gaussian in

character for all molar masses of PEO (Figure 2). This result is an indication that the structure of the matrix appears homogeneous over the length scale investigated. In passing, we note that the rms distances traveled by the PEO in the 1% EHEC matrix range from 1.4 to 10.6  $\mu\text{m}$ . As a result, the discussion from here on refers to center of mass motion. The diffusion coefficient follows a power law dependence on the molar mass as shown in Figure 3. From the slope we find  $\alpha = 1$ . This result is generally ascribed to the Rouse behavior (dilute chain without hydrodynamic interactions). Thus, the PEO dynamics follows that of a Rouse chain due to the matrix screening of the hydrodynamic interactions.

Turning to the echo decays for PEO in the 1% EHEC gel, we note that the results are somewhat different. As can be seen in Figure 5, the echo decays for all PEO's are curved when plotted in a Stejskal–Tanner plot, which indicates a propagator that is not Gaussian, an effect that we suggest originates from the heterogeneities of the matrix. The main difference between the gel and the solution is that the matrix structure is fixed in the gel. In the solution, the matrix structure continuously forms and breaks (although the speed of breaking and forming is not fast enough to average the diffusion for the EHEC polymer itself, as shown in a previous paper<sup>14</sup>), and apparently this makes the PEO diffusion Gaussian in character. When the solution is freezed into a gel, a static network is formed. In this case, we can only speculate on the reason for the curvature in the echo decays. The first situation that becomes apparent is due to the matrix heterogeneity. Because the gel is heterogeneous, PEO will diffuse differently because of the difference in topological constraints depending on the location of the PEO. On the time scale of the experiment the PEO will not have a chance to experience all space. Although the matrix is very heterogeneous, the propagator is still Gaussian in character. Consequently, this can give rise to the observed echo decay. The other reason for the curved echo decays can be due to a non-Gaussian propagator. A situation that would most probably be the case if the EHEC gel was such that it formed pores. PEO residing in such pores would experience hindered diffusion, and consequently this would affect the propagator and could give rise to curved echo decays.

One important result is seen in the low values of  $D/D_0$  as shown in Figure 4. Although the EHEC concentration is only 1 wt % (which corresponds roughly to a volume fraction of 0.01), this appears to severely obstruct the diffusion of PEO. One explanation for this result could be specific interactions between EHEC and PEO. However, previous results on nonionic micelles of the  $C_m\text{-EO}_n$  type have shown that there is only a very weak interaction between the headgroup of the surfactant (which consists of a PEO chain) and the EHEC polymer. Another explanation, which will be discussed in more detail below, is the strong dependence of the mean-square displacement on the molar mass due to matrix inhomogeneities.

Turning to the results from the 6% EHEC solution, we note that the echo decays behave differently than in the 1% EHEC solution and gel. Here the echo decay for the lower molar masses all follow a straight line in the Stejskal–Tanner plot. As the molar mass increases, a fast component is present as indicated by the initially decaying echo. However, the fraction of this component is low for all molar masses except for 963 kDa, where

the fraction is 0.5. The functional form for  $\langle z^2 \rangle$  vs  $M$  also differs from the 1% EHEC case. Previously, we were able to describe this dependence according to a power law scaling. This is not possible here. Concerning the functional form of the  $\langle z^2 \rangle$  dependence on  $M$ , we note some interesting features in comparing the results in Figure 8 with the simulation work by Muthukumar et al.<sup>21–23,27</sup> and the work by Hubert et al., who considered the situation of reptation dynamics in the presence of a random energy landscape.<sup>31</sup> Although they simulated a situation with very strong topological constraints, i.e., high concentrations of obstructing matrix (a situation that is not the case even for the 6% EHEC), we conclude that the same qualitative results can be found here. According to Figure 8, there seem to exist several different regimes of scaling dependencies, most probably due to a change in diffusion mechanism. Although the results in Figure 9 indicate that the diffusion of polymers is governed by Fickian diffusion, we argue that the existence of different scaling regimes is an effect arising from matrix heterogeneity. It is no surprise that stronger scaling exponents are present for the higher matrix concentration. However, we note that for low molar masses  $\alpha \approx 0.9$ , a value that is even smaller than that found for the lower EHEC concentrations. This is an unexpected result, for which we have no current explanation. An even more unexpected result is found at the higher molar masses of PEO, where  $\alpha \approx 0.9$ . Considering the high concentration of matrix and the high molar mass of PEO, this value is unexpectedly small. We can only speculate on the reason for this behavior, referring again to the effect of entropic trapping. Specifically, we note that one important result from computer simulations of polymer dynamics in heterogeneous media is that the polymer chain has been found to shrink.<sup>27</sup> The shrinkage for large molar masses has been shown to be proportional to  $M^{-1}$ .

For the intermediate molar masses  $\alpha \approx 2$ . As previously mentioned, this value is high considering the matrix concentrations and molar mass. We interpret this as an effect of the strong scaling dependence in this regime, the appearance of which is due to the presence of entropic traps<sup>21–23,27</sup> that act as bottlenecks for the diffusion of PEO.

## Conclusions

We have shown that the echo decays for PEO diffusing in a solution matrix of EHEC show Gaussian diffusion behavior for the molar mass range investigated here. This was noted for both 1% and 6% EHEC. When the 1% solution structure was frozen, by chemical cross-linking of the polymer, the echo decays showed a more complex behavior. Even for the lowest molar mass of PEO there was a curvature in the echo decay. The curvature became more pronounced as the molar mass of PEO was increased.

In both solution and gel, power scaling of  $D$  with  $M$  gave a scaling exponent close to 1; i.e., the PEO behaved as a Rouse chain in the 1% EHEC matrix. Considering that the volume fraction of EHEC matrix is only 1%, the obstruction of PEO is very large ( $D/D_0 \approx 0.3$ ). We interpret this results as a result of the fact that, according to computer simulations,<sup>27</sup> the diffusion in random media is slower due to the presence of entropic traps that act as bottlenecks for the PEO transitional dynamics.

When the EHEC concentration was increased to 6%, the scaling of  $\langle z^2 \rangle$  with  $M$  showed an interesting behav-

ior. The functional form no longer followed a power type law but rather involved several regimes. The result showed that  $0.9 < \alpha < 2$ . For the low molar masses the smallest value of  $\alpha$  was found to be 0.9. When the molar mass was increased,  $\alpha$  increased to 2. When the molar mass was further increased,  $\alpha$  decreased to 0.9. (Although the scaling results are limited to include only a few points in the high and low molar mass regime, it is our belief that the quality of the data is such that the results are significant.) This is a very unexpected result. Although we are not equipped with a model for the diffusion behavior observed, we believe that the different scaling regimes reflects a change in diffusion mechanism as a result of diffusion in a heterogeneous medium.

**Acknowledgment.** Valuable discussions with Kristofer Thuresson are gratefully acknowledged. This work was financially supported by the Swedish Natural Science Research Council and by the Center for Amphiphilic Polymers. The NMR spectrometer used was bought with a grant from the Swedish Council for Planning and Coordination of Research.

## References and Notes

- (1) Carlsson, A.; Lindman, B.; Nilsson, P.-G.; Karlsson, G. *Polymer* **1985**, *27*, 431–436.
- (2) Carlsson, A.; Karlström, G.; Lindman, B.; Stenberg, O. *Colloid Polym. Sci.* **1988**, *266*, 1031–1036.
- (3) Lindell, K. In *Physical Chemistry I*; University of Lund: Sweden, Lund, 1996.
- (4) Nilsson, S.; Holmberg, C.; Sundelöf, L.-O. *Colloid Polym. Sci.* **1994**, *272*, 338–347.
- (5) Nilsson, S.; Holmberg, C.; Sundelöf, L.-O. *Colloid Polym. Sci.* **1995**, *273*, 83–95.
- (6) Nilsson, S. *Macromolecules* **1995**, *28*, 7837, 7844.
- (7) Nyström, B.; Walderhaug, H.; Hansen, F. K. *J. Phys. Chem.* **1993**, *97*, 7743–7752.
- (8) Holmberg, C.; Nilsson, S.; Singh, S. K.; Sundelöf, L. O. *J. Phys. Chem.* **1992**, *96*, 871–876.
- (9) Thuresson, K.; Nyström, B.; Wang, G.; Lindman, B. *Langmuir* **1995**, *11*, 3730–3736.
- (10) Thuresson, K. *J. Phys. Chem.* **1995**, *99*, 3823–3831.
- (11) Thuresson, K. in *Physical Chemistry I*; University of Lund: Sweden, Lund, 1996.
- (12) Thuresson, K.; Nilsson, S.; Lindman, B. *Langmuir* **1996**, *12*, 530–537.
- (13) Thuresson, K.; Söderman, O.; Hansson, P.; Wang, G. *J. Phys. Chem.* **1996**, *100*, 4909–4918.
- (14) Nydén, M.; Söderman, O. *Macromolecules* **1998**, *31*, 4990.
- (15) Walderhaug, H.; Nyström, B. *Macromolecules*, in press.
- (16) Rosén, O.; Piculell, L. *Polym. Gels Networks* **1997**, *5*, 185–200.
- (17) Callaghan, P. T. *Magn. Reson. Imaging* **1996**, *14*, 701.
- (18) Stejskal, E. O. *J. Chem. Phys.* **1965**, *43*, 3597.
- (19) Callaghan, P. T.; Coy, A.; MacGowan, D.; Packer, K. J.; Zelaya, F. O. *Nature* **1991**, *351*, 467–469.
- (20) Doi, M.; Edwards, S. F. *The Theory of Polymer Dynamics*; Oxford Science Publications: New York, 1986.
- (21) Muthukumar, M.; Baumgärtner, A. *Macromolecules* **1989**, *22*, 1937–1941.
- (22) Muthukumar, M.; Baumgärtner, A. *Macromolecules* **1989**, *22*, 1941–1946.
- (23) Muthukumar, M. *J. Non-Cryst. Solids* **1991**, *131–133*, 654–666.
- (24) Johansson, L.; Elvingsson, C.; Löfroth, J.-E. *Macromolecules* **1991**, *24*, 6024.
- (25) Cukier, R. I. *Macromolecules* **1984**, *17*, 252–255.
- (26) de Gennes, P. G. *Scaling Concepts in Polymer Physics*; Cornell University: Ithaca, NY, 1979.



- (27) Baumgärtner, A.; Muthukumar, M. *J. Chem. Phys.* **1987**, *87*, 3082–3088.
- (28) Rotstein, N. A.; Lodge, T. P. *Macromolecules* **1992**, *25*, 1316.
- (29) Lodge, T. P.; Rotstein, N. A. *J. Non-Cryst. Solids* **1991**, *131–133*, 671–675.
- (30) Slater, G. W.; Wu, S. Y. *Phys. Rev. Lett.* **1995**, *75*, 164–167.
- (31) Hubert, S. J.; Krzywinski, M.; L'Heureux, I.; Slater, G. W. *Macromolecules* **1998**, *31*, 181.
- (32) Thuresson, K.; Lindman, B. *J. Phys. Chem.* **1997**, *101*, 6460–6468.
- (33) Waggoner, A. R.; Blum, F. D.; Lang, J. C. *Macromolecules* **1995**, *28*, 2658–2664.
- (34) We note that the use of PEO as probe for the EHEC microstructure was recently used by Walderhaug et al.<sup>15</sup> However, the system under investigation in that paper was a mixture of surfactant and polymer, and the molar mass range was limited to two different molar masses.

MA981067Y